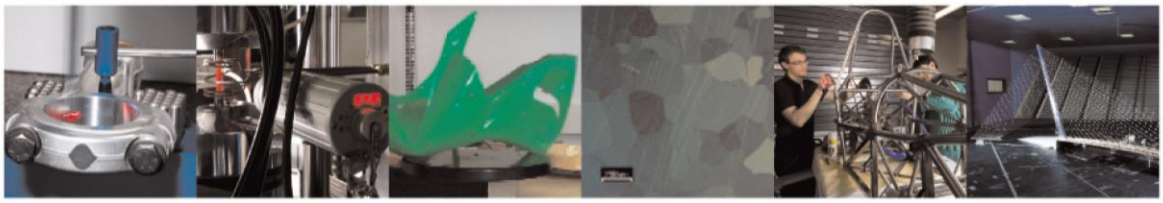

A cyber-physical system for quality-oriented assembly of automotive electric motors

Colledani, M.; Coupek, D.; Verl, A.; Aichele, J.; Yemane, A.

This is a post-peer-review, pre-copyedit version of an article published in CIRP - JOURNAL OF MANUFACTURING SCIENCE AND TECHNOLOGY. The final authenticated version is available online at: http://dx.doi.org/10.1016/j.cirpj.2017.09.001

DIPARTIMENTO DI MECCANICA ■ POLITECNICO DI MILANO
via G. La Masa, 1 ■ 20156 Milano ■ EMAIL (PEC): pecmecc@cert.polimi.it
http://www.mecc.polimi.it
Rev. 0

A Cyber-Physical System for Quality-Oriented Assembly of Automotive Electric Motors

M. Colledani[1,2], D. Coupek[3], A. Verl[3], J. Aichele[4], A. Yemane[1]

[1]Politecnico di Milano, Department of Mechanical Engineering, Via la Masa, 1, 20156, Milan, Italy.
[2] ITIA-CNR, Institute of Industrial Technologies and Automation, Via Bassini 15, 20133, Milan, Italy
[3]Institute for Control Engineering of Machine Tools and Manufacturing Units (ISW), Seidenstraße 36, 70174 Stuttgart, Germany.
[4]Corporate Research Robert Bosch GmbH, Postfach 300240, 70442 Stuttgart, Germany

Abstract
The production of motors for the electric vehicles requires innovative and systematic quality control approaches to boost efficiency while moving from low volume towards mass production. In this context, end-of-line quality testing methods are usually applied to assess the product functionality at the end of the process chain. However, this approach does not allow process monitoring and the in-line prevention and correction of defects, leading to significant scrap rates and value losses.
This paper presents a new system-level strategy for the in-line quality-oriented assembly of rotors in the production of automotive electric drives. The new strategy is based on a new cyber-physical system that optimizes the assembly strategy depending on the quality of magnetized stacks, monitored with data gathered by in-line inspection. For each batch, the magnetic stacks to be assembled and their orientation is selected according to an optimization algorithm, aiming at minimizing the deviation from the target total integral magnetic flux and maximizing the field uniformity in the magnetized rotor. The impact of the proposed strategy on the quality and productivity related performance measures are predicted by analytical methods. Experimental results based on an industrial case study are reported, showing that the application of the proposed strategy yields a significant increase in the production rate of conforming engines. The proposed approach paves the way to innovative zero-defect manufacturing strategies at system level in emerging, high-tech, manufacturing sectors.
Keywords: Assembly, Quality, Productivity, Electric vehicle, Electric motor, Cyber-Physical Systems.

1. Introduction

Sustainable mobility is one of the most important challenges towards a low carbon economy and a more sustainable society. According to the 'European Roadmap for Moving to a Competitive Low-Carbon Economy in 2050', transportation is one of the most relevant sectors for reducing emissions [1]. This sector accounted for 16% of the total global emissions in 2015 [2]. In order to reduce emissions of the current car fleet, the trend is going towards zero-emission vehicles using electric motors [3]. Recent studies show the huge potential of electric motors in replacing combustion engines (petrol and diesel), in particular for medium-sized cars [4]. Following these trends, a requirement to move from small series to mass production of electric motors is observed in the automotive sector, for hybrid and purely electric vehicles. Governmental regulations and targets for increasing the amount of electric vehicles accelerate this development [5,6]. In this favourable context, the market growth of electric vehicles is, however, strongly constrained by the availability of advanced manufacturing technologies and methods able to support their production at affordable prices. Therefore, efficient production and quality control strategies play a significant role to boost an economically and environmentally sustainable transition to mass production of electric vehicles.

In the current production scenario, end-of-line quality testing strategies are usually applied to assess the product functionality before delivering the electric drive to the market [7,8]. At the end of the process-chain, the functionality of the assembled motor is tested, in terms of power, torque, and absence of cogging, yielding to a classification into conforming and non-conforming parts. Non-conforming parts are either disassembled and reworked, or scrapped. Both actions entail a significant operational cost due to material losses and non-value-adding processes. To avoid these problems, manufacturers usually apply wide tolerance limit widths and a conservative motor design [8]. In other words, large variability in the product performance is accepted and the target requirements are met by oversizing the product by design. An

alternative cost-effective strategy would be to smooth the product performance variability by implementing process monitoring and in-line prevention of defects, before the product reaches the final stage of the process-chain. To this aim, innovative quality control methods and strategies for avoiding the generation and propagation of defects along the stages of the production line need to be introduced, with the objective to move towards the zero-defect manufacturing paradigm in this strategic industrial sector.

In literature, only few approaches try to overcome the drawbacks of the current end-of-line quality control solution in the production of electric drives for the e-mobility sector. The majority of the approaches focus on the critical process stage of rotor magnetization and rely on the inspection of single magnets. For example, in [8] the authors propose the inspection of single permanent magnets after magnetization, by storing them in an automated warehouse system next to the assembly station. The advantage of this approach is that the actual magnetization of the permanent magnets is individually measured and compared to the set-point. However, this approach is usually too conservative and results in high scrap rates, since the opportunity to obtain conforming rotors by a proper combination of magnets with highly deviating magnetization levels is neglected. In addition, there are several drawbacks while handling magnetized materials, e.g. restrictions in transportation, contamination of the magnets and operators' safety [9]. For these reasons, permanent magnets are mostly magnetized after assembly. Inspection of permanent magnets before magnetization and assembly are described in several papers [10–13]. However, this strategy introduces an additional handling and inspection station into the production line, increasing costs and line complexity and shifting the quality problem to the magnet suppliers, thus increasing their costs.

Emerging Key Enabling Technologies (KETs), such as in-line data gathering solutions, data storage and communication standards, data analytics tools and digital manufacturing technologies offer new opportunities for zero-defect manufacturing, in complex production environments. These technologies are increasingly becoming integral part of modern production systems [14]. If these technologies are properly integrated with a cross-KETs approach, new Cyber-Physical Systems (CPSs) can be designed and implemented at shop floor level, to support systemic zero-defect manufacturing solutions [15].

CPSs are usually defined as systems integrating computation and physical actuation capabilities [16]. In CPSs, embedded computers and networks monitor and control physical processes, usually with feedback loops, where physical processes affect computations and vice versa [17]. Innovative applications of CPSs for improving manufacturing efficiency and responding to emerging industrial problems is attracting the interest of both industries and researchers [18]. This trend is transforming the manufacturing industry to the next generation, namely the fourth industrial revolution "Industry 4.0" [16]. It envisions the promise to couple the world of production and network connectivity into an "Internet of Things" to realize "Smart production" as the new norm in a world where intelligent ICT-based machines, systems and networks are capable of independently exchanging and responding to information to manage industrial production processes [19]. This potential in connectivity and computational power in manufacturing can also be exploited to support the implementation of efficient in-line quality-oriented production solutions [20].

This paper proposes a new quality-oriented strategy for the assembly of electric motors in the e-mobility industry. The solution is based on a CPS that optimizes the assembly strategy depending on the quality of magnetized stacks, monitored with data gathered by in-line inspection. For each batch, the magnetic stacks to be assembled and their orientation is selected according to an optimization algorithm, aiming at maximizing the field uniformity in the magnetized rotor. An analytical method for the analysis of percentage of conforming rotors, total production rate and work in progress of the system operating under this new assembly strategy is developed. The proposed solution is validated with real data obtained from Robert Bosch GmbH, as one of the Use Cases of the *MuProD* project, funded by the European Union [21,22]. The experimental results show that the application of the proposed strategy yields a significant increase in the production rate of conforming engines.

The paper is organized as follows: Section 2 describes the process chain of the Bosch electrical motor assembly line. Section 3 introduces the design of the CPS solution and the techniques for the measurement and estimation of two key quality characteristics of the rotor. Section 4 describes the proposed methods for enabling a quality-oriented rotor assembly by considering the two key quality characteristics. Section 5 presents an evaluation method for estimating the output performance measures of the system operating under the new assembly strategies. Section 6 describes the implementation architecture and discusses the demonstration of the proposed solution in real industrial settings.

2. Description of the production system

In this section, the Bosch electrical motor production line for permanent-magnet synchronous motors, that are widely spread in the automotive industry, is described [23,24]. The rotor of such an electrical motor consists of S_P stacks. Each stack contains M_P permanent magnets radially embedded in a circular steel ring. By piling several stacks together, rotors of different torque can be produced with the same cross-section. The production line is composed of three main branches, namely rotor assembly, stator and housing production (Fig. 1). In the figure, light blue squares represent processing stages, red squares represent inspection stages and circles represent buffers for temporarily storing in-process inventory. In this paper, the analysis is focused on the rotor line that is composed of seven main stages, described in the following:

- M_1: loading of the stacks on the pallet.
- $M_{2,1}$, … $M_{2,x}$: assembly of the embedded permanent magnets on the stacks.
- M_3: stack magnetization process and inspection.
- M_4: heating station for glue drying.

- M_5: rotor assembly machine.
- M_6: rotor balancing station.
- M_7: rotor marking station.

After the motor is assembled in M_g, it undergoes a final quality control at the end of line (EOL) inspection station, M_k [7]. Two key quality characteristics are inspected. First, the overall magnetic moment of the motor should be within a tolerance limit of 4% from the target value. Secondly, the motor should be free from significant cogging and vibration. The main drawback of the current inspection is that it is performed at the final stage of the manufacturing line, where defects cannot be corrected [23,25]. Consequently, a defective motor can only be recycled, by disassembly, or scrapped, with significant value losses [26].

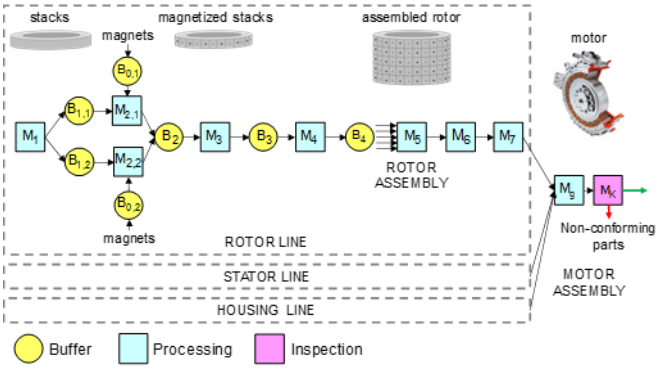

Fig. 1. Schematic view of a rotor production line for permanent-magnet synchronous motors in the automotive industry.

3. Design of the CPSs solution

The overall CPS-based assembly solution proposed in this paper is divided into three main steps, as shown in Figure 2. The first step involves the identification of product critical quality characteristics and the development of a new inspection technique for their measurement. Thus, it introduces a pre-assembly inspection technique for stacks and the estimation of two key quality characteristics of the rotor. The second step develops optimization techniques for the improvement of the two key quality characteristics by using the information from the newly developed inspection station. The third step proposes an analytical evaluation methodology for predicting the integrated quality and production logistics effects of the new assembly solution. The system level modelling of the production system considers the changes due to the introduction of the new inspection station (developed in Step 1) and the implementation of optimization techniques (developed in Step 2). Finally, a pilot test setup of the solution integrating the required hardware and software components is built to validate the applicability of the solution on a real industrial setting.

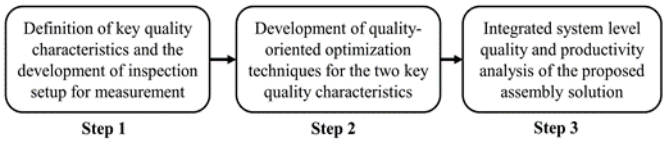

Fig. 2. Main steps of the overall CPS-based approach

In this section, the two key quality characteristics are identified and their impact on the operational performance of the motor is discussed. Then, a newly proposed inspection test bench set-up for the space-resolved measurement of stack magnetization profile is described. The data gathered about the magnetization profile of stacks are used to estimate the two key quality characteristics. Then mathematical procedures that transform the stack magnetization profile measurements into values that will be used for the estimation of the two key quality characteristics of the rotor are formulated.

3.1. *Key product quality characteristics*

By considering the main factors that impact the operational performance of the rotor, two key quality characteristics (*KQC*) are considered. The first one is the *total integral magnetic flux* (KQC_1) of the rotor and the second one is the *uniformity of magnetic field intensity* (KQC_2) of the rotor. Both *KQCs* influence the operational performance of the final assembled electric motor. The total integral magnetic flux of a rotor determines the motor's capability to generate the target design torque, while the uniformity of the magnetic field intensity allows the motor to run without cogging, excessive vibration and noise [27].

3.1.1. Total integral magnetic flux (KQC_1)

The target design torque (τ_{tar}) is specified depending on the model of the motor. The total integral magnetic flux determines the average torque that can be generated by the motor. Currently the maximum acceptable deviation of the torque from the target value is ±4%. Thus, the total integral magnetic flux of a rotor (Φ_{tar}), must comply with this tolerance limit. The variability generated by the magnetization process creates a variation on the magnetic flux of stacks. Thus the integral magnetic flux of the assembled rotor from the variable stacks creates a deviation from the target value. The actual integral magnetic flux can be measured after the rotor is completely assembled. On the other hand, it can also be estimated (Φ_{est}) before the assembly process using the total flux measurements from inspected stacks [28,29]. This study is based on the latter approach, which introduces a pre-assembly inspection of stacks, in order to implement an optimized assembly strategy.

3.1.2. Uniformity of magnetic field (KQC_2)

A uniform magnetic field intensity profile of the rotor is a desirable characteristic in order to avoid potential cogging, vibration and noise generated during the operation of the motor [27]. The variation between magnetic field intensity of individual magnets on a single stack arises from the magnetization process and the material properties [30,31]. This leads to a variation in the magnetic field intensity profile of a stack. However, during the assembly process the variation of the average magnetic field intensity profile in the assembled rotor can be minimized by creating the proper alignment between the stacks. The reduction in the variation of magnetic field intensity of the rotor is achieved by aligning a stronger magnet on one stack positioned against to a weaker magnet on

another stack so that the average magnetic field intensity across a column of magnets is compensated.

3.2. *New inspection station for the magnetic field profile*

The two quality characteristics, i.e., KQC_1 and KQC_2 depend on two main factors, namely the magnetic field intensity profile of individual stacks generated by the magnetization process (M_3), and the rotor assembly process which assembles stacks into a rotor (M_5). In the current system configuration, the magnetization process (M_3) is considered as a black box and cannot be controlled. Therefore the goal of this study is to improve the quality of the rotor during the assembly operation. This approach requires the measurement of magnetic field intensity of the individual stacks after the magnetization process. The measurement information is an input for decision making on an optimal assembly process. As a consequence, devising appropriate inspection techniques for the measurement of magnetic field intensity of stacks is required. The reference principles for magnetization inspection are magneto-optical sensors [32], search coils [33] and hall sensors [34–36]. The proposed pre-assembly inspection of stacks allows overcoming the drawbacks of the currently applied EOL inspection. The new inspection technique enables the measurement of the space resolved magnetic field intensity of individual stacks before the rotor assembly is performed. Therefore, an inspection test bench equipped with devices for measurement of magnetic field profile intensity and communication tools for data transfer to a computer is developed. The computer is equipped with software tools for the analysis of the acquired data and the estimation of the two *KQCs*.

3.2.1. Inspection test bench setup and measurement

The principal setup of the inspection test bench designed and developed for this purpose is depicted in Fig. 3. The inspection test bench includes three linear axes, one rotational axis, a pneumatically operated three finger gripper, a system for permanent distance control and a newly developed sensor for monitoring the magnetic field [37].

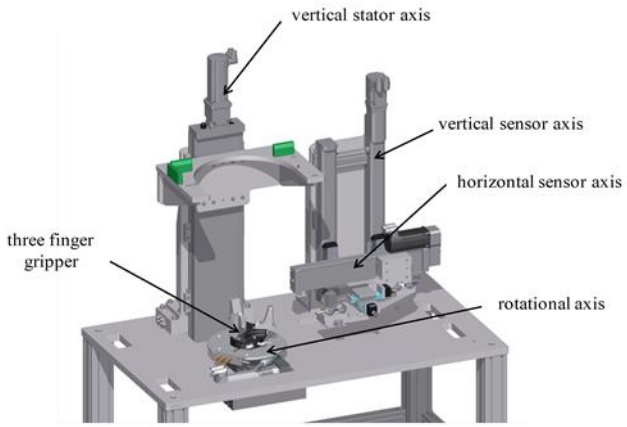

Fig. 3. Principal set up of the test bench for space-resolved inspection of single stacks and assembled rotors [37].

For the space resolved inspection of a steel stack, the stack is clamped on the three-finger gripper. Subsequently, the magnetic sensor and the distance control are positioned by moving the sensor axes. The distance between the sensor and the stack is determined during preliminary experiments considering the operating curve and the sensitivity of the magnetic sensor. The actual measurement process is conducted by considering acceleration and deceleration effects of the rotational axis. The stack rotates with constant velocity while the magnetic sensor remains in its position.

Fig. 4 shows the space-resolved measurement of the magnetic flux density of a steel stack with $M_P = 24$ embedded magnets. Tolerances due to the production process on the shape of the stacks as well as misalignment effects in the setup of the test bench induce fluctuations in the distance between the magnetic sensor and the stack. This directly correlates with the intensity of the measured magnetic field, a permanent distance, and therefore eccentricity control is necessary. Thus the test bench is equipped with a sensor for contact-free distance monitoring. By analysing and processing this data, online eccentricity compensation is possible [37].

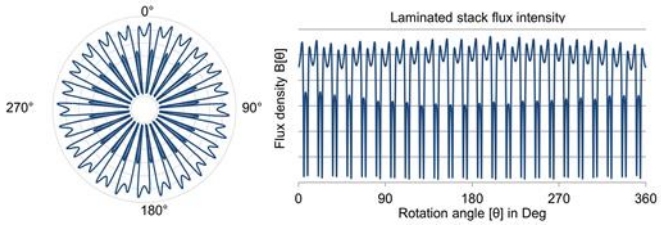

Fig. 4. Flux density of a steel stack with 24 buried permanent magnets.

3.2.2. Estimation of magnetic flux of stacks

The data acquired from the inspection test bench is a continuous space resolved measurement of the magnetic field intensity profile of single stacks. This continuous measurement needs to be transformed into discrete values per magnet in order to simplify the estimation and optimization of the *KQCs*. Therefore, this section presents a mathematical procedure for transforming the continuous measurements into one value per magnet, i.e., vector of M_p values per stack. The discretized values are the input for the optimization of the *KQCs* of the rotor presented in Section 4.

The average magnetic field intensity profile of a magnet *j* on circular stack *i*, $B_{i,j}$ is evaluated from the space resolved magnetic field intensity profile $B[\theta]$ (Fig. 4). The angular distance covered by a single magnet is equal to $2\pi/M_P$ rad ($360/M_P$) degrees. For a stack with 24 magnets, this angular distance is equal to $\pi/12$ rad (15°) and the corresponding average magnetic flux can be computed as:

$$B_{i,j} = \frac{\int_{\theta=(j-1)*\pi/12}^{j*\pi/12} B[\theta].d\theta}{\pi/12}, \ \forall\ j = 1,...,24. \quad (1)$$

Equation (1) transforms the continuous measurement obtained in Fig. 4 into a vector of 24 values corresponding to each

magnet on a stack as shown in Fig. 5. Based on these values the average magnetic field intensity of each magnet can be computed. The area normal to each magnet is $A_{i,j}$ and it can be assumed equal for all magnets A. Thus, the magnetic flux across a single magnet is evaluated as the product of the average magnetic field intensity and this cross section area as:

$$\phi_{i,j} = B_{i,j} \times A \tag{2}$$

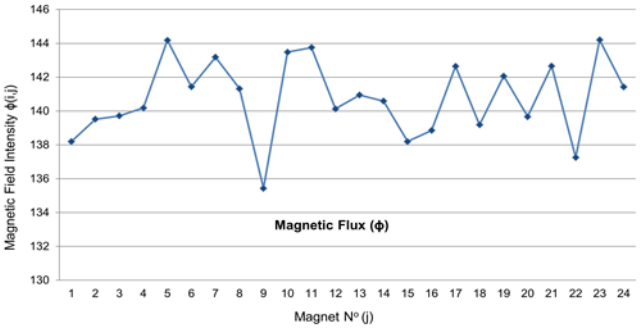

Fig. 5. Average magnetic field of 24 magnets on a stack.

By using the vector of magnetic flux of each stack, the total integral flux (Φ_{est}) of a rotor assembled from S_p stacks can be estimated as:

$$\Phi_{est} = \sum_{i}^{S_p} \sum_{j}^{M_p} \phi_{i,j} \tag{3}$$

In order to measure the uniformity of the magnetic flux of a rotor (Fig. 6) constructed from S_p stacks the magnetic flux ϕ_j of the magnets on that column j needs to be evaluated. This quantity can be approximated as (4). The goal is to keep the ϕ_j closer to the target value by positioning positive and negative deviations of magnets in the same column.

$$\phi_j^M = \sum_{i=1}^{S_p} \phi_{j,i} \tag{4}$$

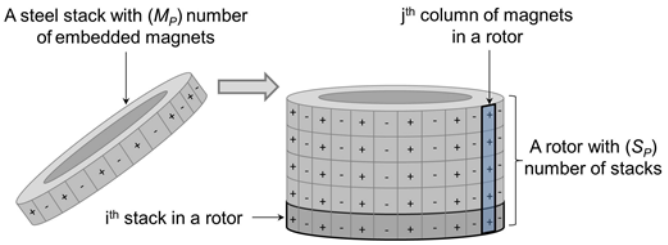

Fig. 6. Schematic representation of stacks and rotor.

On the other hand, the integral magnetic flux across a single stack can be computed as:

$$\phi_i^S = \sum_{j=1}^{M_p} \phi_{j,i} \tag{5}$$

The extended description of the mathematical methods to achieve optimal compensation strategy is given in the next section.

4. In-line quality optimization methods

In this section, optimization techniques that consider each of the two key quality characteristics *KQCs* are presented. Separate optimization techniques are developed based on the target key quality characteristics; KQC_1 for total integral magnetic flux and KQC_2 for the uniformity of magnetic field.

4.1. *Optimization of KQC_1 (Total integral magnetic flux)*

The goal of optimizing KQC_1 is to enable the assembly of a rotor with a total integral magnetic flux value close to the target (Φ_{tar}), given a set of available stacks for assembly. There are different approaches that can be applied for the optimization of KQC_1. In this study, a direct selective assembly technique is chosen. The technique is based on the estimated magnetic flux of stacks presented in Section 3. Individual stack inspections are used to calculate the deviations from target reference values for single stack (ϕ_{tar}^S) and this information is used to minimize the cumulative deviation on the reference target value of the output rotor (Φ_{tar}). Considering the Φ_{tar} of a rotor with S_p stacks, the nominal target magnetic flux for stacks and for magnets can be calculated as ϕ_{tar}^S and ϕ_{tar}^M respectively. Therefore, the deviations of magnetic flux for each stack and each magnet from these nominal values can be computed.

In the direct selective assembly, the selection is performed on the available set of stacks after the magnetization station. Considering the number of stacks for a rotor is S_P, then assembly can be done when there are S_{Av} available stacks which is equal or greater than S_P. The number of combinations that need to be evaluated are $C(S_{Av},S_P)$. The goal is to find the optimal combination of k_{opt} stacks with cardinality of S_P that minimizes the deviation from the target total integral flux of the rotor Φ_{tar}. If C is the combinatorial set of the available stacks S_{av}, then the objective equation can be expressed as:

$$\Delta\Phi^R(k) = |\sum \Delta\phi^S{}_i| \text{ for all } i \in k. \tag{6}$$

Then optimal k_{opt} is:

$$\Delta\Phi^R(k_{opt}) = \min \{\Delta\Phi(k)| \, k \in C\} \tag{7}$$

For instance if there are 10 stacks available (S_{av} = 10) for assembling a rotor of 5 stacks (S_P = 5), the rotor can be constructed from a possible set of 252 combinations. Therefore, the goal is to find the optimal combination C_{opt} of the stacks that minimizes the deviation of target total integral flux.

4.2. *Optimization of KQC_2 (uniformity of magnetic field)*

The optimization techniques proposed for KQC_2 aim to improve the uniformity of the magnetic field profile of a rotor closer to a given reference value (ϕ_{tar}^M). Magnetic profile uniformity is influenced by manipulating two decision variables that define the relative arrangement of stacks. The first variable determines the relative angular alignment between stacks and the second is related to the vertical

arrangement of the stacks. The optimization techniques are also presented based on these two variables.

The two step approach considers one decision variable (one step) at a time. In this approach, we present how the two steps are mathematically formulated and evaluated. Step 1 changes the angular alignment of stacks, and Step 2 manipulates the vertical order of stacks in order to improve the uniformity of magnetic profile of the rotor.

4.2.1. Step 1: Angular orientation optimization.

The aim of this step is to impose an angular misalignment α between the stacks with respect to a reference axis in order to gain uniformity and reduce variability of the output field intensity. The entity of this misalignment, namely the elements of the vector α, have to be computed by an optimization algorithm. The optimization problem is the minimization of a dispersion metrics calculated between the magnetic field intensity of the rotor. According to the representation of the rotor as a matrix, the aim is to change α in order to compensate the accumulated deviations in the corresponding column. Values of vector α are integers indicating the counter clockwise shift of a magnet pair, in the same row. After $M_P/2$ shifting operations the stack reaches its starting position. Therefore, α is defined as follows:

$$\vec{\alpha} = \begin{bmatrix} \alpha_1 \\ \vdots \\ \alpha_{S_P} \end{bmatrix} \qquad \text{with } 0 \le \alpha_i < \frac{M_P}{2} \quad \forall i \qquad (8)$$

In order to avoid redundant permutations, the first stack is not shifted and can be seen as fixed reference for the shifting operations of the remaining S_P-1 stacks ($\alpha_1 = 0$). During the execution phase, the optimization algorithm has to be evaluated for each specific batch of S_P stacks to be assembled in order to compute the specific assembly policy. At this step, it is assumed that the choice of our dispersion metrics is the first order i.e., absolute difference not variance. Therefore, from the space resolved measurement we compute the individual deviations as:

$$\Delta\phi_m = \sum_{j=1}^{M_P} \left| \phi_j - \phi_{tar}^{M} * S_P \right| \qquad \text{where} \quad \phi_j = \sum_{i=1}^{S_P} \phi_{j,i} \qquad (9)$$

In order to find the best solution with the underlying cost function, the total magnetization deviation $\Delta\Phi(\alpha_i)$ is computed for each fixed rotation and stored together with the corresponding rotation vector α_i. Formally, each instance of this combinatorial optimization problem can be formulated as pair $(\Omega, \Delta\Phi)$, where Ω is the set of all feasible solutions and $\Delta\Phi$ is a mapping $\Delta\Phi : \Omega \rightarrow R$ that assigns a scalar cost value to each element from the set Ω. The goal of finding an optimal rotation α_{opt} for which the flux deviation $\Delta\Phi(\alpha_{opt})$ becomes minimal. A brute-force algorithm searches for the global minimum $\Delta\Phi(\alpha_{opt})$ in the entire solution space Ω:

$$\Delta\Phi(\vec{\alpha}_{opt}) = \min\left\{\Delta\Phi(x) \mid x \in \Omega\right\} \qquad (10)$$

During the execution phase, the combinatorial optimization problem stated in equation (9) (angular orientation) has to be solved for each specific batch of S_P stacks to be assembled in order to compute the specific assembly policy. Therefore, the computation time directly interferes with the cycle time and should be minimized. The number of possible permutations π^{all} in the solution space Ω grows exponentially with the number of stacks:

$$\pi^{all} = \left(\frac{M_P}{2}\right)^{S_P - 1} \qquad (11)$$

As the brute-force algorithm searches for the global minimum of all permutations, its computation time grows when increasing the solution space. Experiments show that the relation between computation time and number of permutations is linear. Thus, the computation time grows exponentially with respect to S_P. The computation time of the brute force algorithm was measured by varying number of stacks S_P on a regular computer (Table 1).

Table 1: Number of permutations and computation times for angular orientation optimization (Step 1).

S_P	M_P	Permutations [-]	Computational effort [s]
3	24	144	0,0010
4	24	1.728	0,0120
5	24	20.736	0,1564
6	24	248.832	1,9603
7	24	2.985.984	25,0890
8	24	35.831.808	319,9934

4.2.2. Step 2: Stack order optimization.

Once the solution of *Step 1* is determined, *Step 2* aims to find the best arrangement of the stacks with respect to their axial positions. The axial order of stacks in a rotor is defined by a vector ρ that indicates the vertical arrangement of the stacks. This vector starts at one for the top stack and then increases to the stack at the bottom. Thus, the size of this vector is equal to the number of stacks in the rotor S_p. The axial arrangement vector ρ has to be optimized such that the variability of the output field intensity of one rotor is reduced. This variability ΔP is modelled as a cost function whose parameters are estimated from experimental observations. The experimental observations are based on two main factors that influence the magnetic field intensity of the output rotor. Consequently the cost function is defined as the superimposition of these two separate factors that are discussed here.

The first experiment is conducted by using stacks with variability to investigate the impact of stack position on the variability of the output field intensity of a rotor. A cost parameter $\Delta P(\rho^{G1})$ as a function of axial position ρ is associated to the variability of the magnetization deviation of stacks. The accumulated variability ΔP_i of a given stack i is computed as the sum of absolute deviations of each magnet on a stack from a fixed reference value of ϕ_{tar}^{M}. In order to measure the impact of vertical position on magnetic flux deviation an empirical

experiment has been conducted. The results are reported for an assembled rotor in

Table 2. These prognosis coefficients indicate that magnetic field variability on the rotor is reduced if the highly variable stack is placed at the central position. Similarly, the prognosis coefficients c_i are estimated for each corresponding position i defined by ρ.

$$\Delta P(\rho^{G1}) = \sum_{i=1}^{S_p} c_i.\Delta P_i \text{ where } \Delta P_i = \sum_{j=1}^{m} \left| \phi_{i,j} - \phi_{tar}^{M} \right|, \forall i = 1,...,S_P \qquad (12)$$

Table 2: Prognosis coefficients and relative stack positions.

Position	Estimation	Parameters
Top stack	$\hat{\phi}_{1,j} = \phi_{1,j} + c_t.\phi_{2,j}$	$c_b = 0.071$
Centre stacks	$\hat{\phi}_{i,j} = \phi_{i,j} + c_c.\phi_{i-1,j} + c_c.\phi_{i+1,j}$	$c_c = 0.045$
Bottom stack	$\hat{\phi}_{n,j} = \phi_{n,j} + c_b.\phi_{n-1,j}$	$c_b = 0.071$

The second experimental observation shows that the variability on the rotor is reduced by positioning oppositely deviating magnets of stacks adjacent to each other. Such reduction in variability is achieved by placing a stronger magnet next to a weaker one so that the close proximity creates a neutralization of the interfacing deviations. This adjacent compensation has to be evaluated for (S_p-1) interfaces formed by a rotor assembled from S_p stacks. The resultant deviation at a given interface between stack i and stack $i+1$ ($\Delta P_{i,i+1}$), is computed as (13). The cumulative interface deviations $\Delta P(\rho^{G2})$ is evaluated as a sum of all interface deviations.

$$\Delta P(\rho^{G2}) = \sum_{i=1}^{S_p-1} \Delta P_{i,i+1} \text{ where } \Delta P_{i,i+1} = \sum_{j=1}^{m} \left| \phi_{i,j} + \phi_{i+1,j} - 2\phi_{tar}^{M} \right|, \forall i = 1,...,S_p \qquad (13)$$

The optimal axial arrangement is the one that has a minimal impact on both of the above two goals. Similarly to *Step 1*, this problem can be formulated as pair (Ω, ΔP), where Ω i.e., the set of all feasible axial positions and ΔP is a mapping ΔP: $\Omega \rightarrow R$. Therefore, the algorithm chooses the optimal arrangement ρ^{opt} that minimizes the sum of the two goals (10).

$$\Delta P(\rho^{opt}) = \min\{\Delta P(\rho^{G1}) + \Delta P(\rho^{G2}) \mid \rho \in \Omega\} \qquad (14)$$

Analogous to *Step 1* optimization, the number of possible solutions and the corresponding calculation time on a regular computer was estimated (Table 3). *Step 2* optimization requires significantly less computational effort due to the reduced solution space.

Table 3: Number of permutations and computation times for stack order optimization (Step 2).

S_P	M_P	Permutations [-]	Computational effort [s]
3	24	6	0,00010
4	24	24	0,00016
5	24	120	0,00090
6	24	720	0,00567
7	24	5.040	0,04234
8	24	40.320	0,36007

5. System level performance

In this section, a new configuration of the system is proposed to support the implementation of the new quality-oriented assembly strategy and the benefits of the proposed quality-oriented assembly strategy at system level are quantified. To this aim, a system level model of the rotor production line is developed considering the specific modifications implied by the proposed assembly strategy. This model makes it possible to perform the joint analysis of quality and production logistics performances of the system. In detail, two process chain models are proposed corresponding respectively to the current configuration and the configuration implementing the newly proposed assembly strategy. This is an adaptation of the current configuration at two specific areas that are affected by the application of the proposed assembly strategy. Firstly, an inspection station for the measurement of magnetized stacks is introduced in (Fig. 8) before M_5. Secondly, the additional times required for inspection, optimization and pre-assembly adjustment of stacks, which affect the assembly process are considered.

5.1. *Performance evaluation of the assembly strategies*

A decomposition based performance evaluation method is adopted to analyze the system level quality and production logistic performances of the current strategy and the newly proposed assembly strategy [38]. This method supports the evaluation of a serial manufacturing system that is composed of multiple processing stages (blue) and inspection stages (red) defined as M_k, $k=1,..,K$, separated by intermediate buffers (circles) (Fig. 7). Buffers have the role of decoupling the consecutive stages in the system, thus, can be either inventory storages or automated material handling systems that transport semi-finished parts between machines.

A continuous time-discrete state Markov chain model is used to characterize the behaviour of each processing stage [38,39]. A transition rate matrix λ is defined to model each machine with multiple operational and failure states by means of arbitrarily complex Markovian structures. When the machine is in an operational state o, it processes parts at a rate of μ_0 parts per minute. A breakdown state is simply characterized by μ=0. These processing rates [parts/t.u.] are collected in the quantity reward vector $\boldsymbol{\mu}$. For each operational state a statistical distribution of the processed key quality characteristic y is assumed, namely $f_o(y)$. According to the specification limits imposed by design on the processed feature, the yield is defined for every state o, namely Y_o; these elements are collected in the quality reward vector $\boldsymbol{Y}$. The total fraction of defects generated by the stage is denoted as γ. The performance measures of interest are the following:

- Average total production rate of the system, E^{Tot}, including both conforming and defective parts, observed in output.
- Average effective production rate, E^{Eff}, of conforming parts, observed in output.
- System yield, Y^{system}, that is the fraction of conforming parts produced by the system (E^{Eff} / E^{Tot}).
- *WIP*, which is the total average inventory of the system.

After deriving the characteristic parameters (λ_i, μ_i, Y_i) for each stage, the steady-state probability vector π of the Markov chain and the performance of the stage in isolation, i.e. not integrated in the production line, can be computed:

$$\pi_i \lambda_i = 0 \qquad E_i^{Tot} = \pi_i \times \mu_i^T \qquad E_i^{Eff} = \pi_i \times diag(\mu_i) \times Y_i^T \qquad Y^{M_i} = \frac{E_i^{Eff}}{E_i^{Tot}} \tag{15}$$

The full exposition of this methodology is presented in [40,21,22], however, without considering the application of the typical assembly strategies proposed in this paper. Since the new assembly strategy affects the material flow and the behaviour of stages, this impact has been included in the corresponding processing stage models.

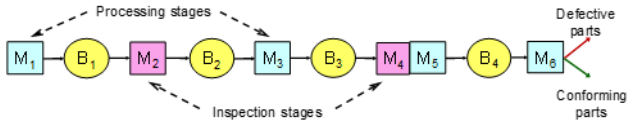

Fig. 7. Modelling formalism for a generic multi-stage production line.

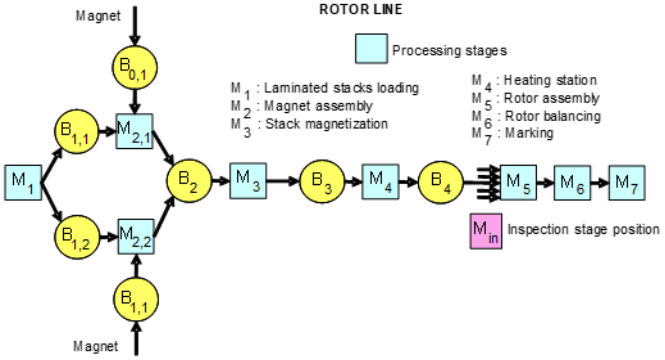

Fig. 8. Current rotor production line and required changes for application of the proposed strategy.

5.2. *Current assembly strategy*

The current assembly strategy is considered as a reference case for comparing the newly proposed quality-oriented assembly strategy. In the process chain (Fig. 9), which corresponds to the current assembly strategy, there are no intermediate inspections since all the inspections are performed at the end of the line.

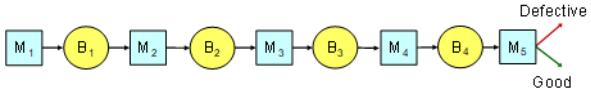

Fig. 9. Approximated process chain of the current production line.

The complex Markovian structure of each machine in this process chain is approximated by using single failure machines. For this reason, an opportune aggregation of their parameters is also performed. The approximated machine parameters are further scaled for the sake of confidentiality and are reported in Table 4. However, these parameters and the related single failure machines are modified depending on the adjustments needed for the proposed assembly strategy.

Table 4: Input parameters used for the rotor production line

Machine ID	Failure rate (p)	Repair rate (r)	Speed μ_o	Buffer ID	Size
M_1	0.002083	6.6667	0.150	**B_1**	5
M_2	0.003333	0.1000	1.800	**B_2**	40
M_3	0.006250	1.0000	0.690	**B_3**	40
M_4	5.71E-06	0.0021	0.667	**B_4**	6
M_5	3.47E-05	0.0067	0.800		

5.3. *Proposed assembly strategy*

The newly proposed assembly strategy configuration optimizes KQC_1 by using the direct selective assembly of rotors from stacks stored in the upstream buffers. The inspection station for the measurement of stacks' magnetization is located downstream the magnetization station, and it is considered integrated to the assembly machine M_5 (Fig. 10). In addition, the configuration of this strategy considers B_3 and B_4 of the original line into a combined single buffer. This modified arrangement allows to generate a higher number of stack combinations for the assembly station M_5, thus increasing the output quality of the assembled rotor. Once the set of stacks are chosen based on the direct selective assembly technique, the two-step approach described in Section 4.2 is applied for optimizing KQC_2 on the selected set of stacks. The computation times required for the direct selective assembly that optimizes KQC_1 are negligible. However, the two-step approach for the optimization of KQC_2 needs a significant computation time. The computation times for the two-step optimization approach (T_{opt}) are estimated using the current buffer level and the values from Table 1 and Table 3. In detail, the following four time quantities are defined and used to compute the parameters of the assembly station under the proposed configuration.

- Assembly time (T_{asbl}) equal to the current process
- Inspection time (T_{insp}) time required by inspection
- Optimization time (T_{opt}) algorithm time
- Additional (T_{add}) time for positioning stacks is considered

By considering these time estimates, the set of transition rates of the equivalent machine M_{dsa} (M_4 and M_5) and corresponding processing rates are computed as follows.

$$p_{dsa} = p \; ; \; r_{dsa} = r \tag{16}$$

$$\frac{1}{\mu_o} = T_{asbl} + T_{insp}; \quad \frac{1}{\mu_{dsa}} = T_{asbl} + T_{insp} + T_{add} + T_{opt} \tag{17}$$

After applying these steps, the modified Markov chain, (Fig. 10 (b)) represents the new model of the approximated equivalent machine M_{dsa} (M_4 and M_5) of the *Strategy 2*.

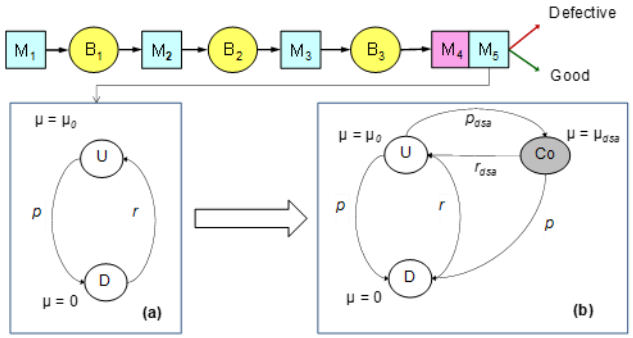

Fig. 10. Process chain model of the direct selective assembly strategy and State transition diagram of stages M_4 and M_5.

5.4. *Numerical results*

Once the modelling adaptations and approximations are done for the two strategies, then the overall performance of the system is evaluated in terms of effective production rate (E^{Eff}). The quantitative models of both the current strategy and the newly proposed strategy are evaluated and the summary of the numerical results are reported in Table 5. The effective production rate (E^{Eff}) is computed as the product of the total production rate (E^{Tot}) and the yield of the system (Y^{system}). The yield of the system indicates the fraction of the conforming rotors with respect to the tolerance limits specified for KQC_1. The outputs numerical results demonstrate that the newly proposed assembly strategy significantly improves the effective production rate of the system. By considering the performance of the current system configuration as a reference case, the effective production rate under the newly proposed strategy has increased by (16.55%). This improvement can be explained through the impacts of the proposed solution on E^{Tot} and Y^{system}. E^{Tot} is slightly lower by 0.3% for the proposed strategy due to the added inspection, optimization and pre-assembly setup times, however, the CPS based optimization technique improves the system yield from the current value of 0.93 to ~1.00.

Table 5: Output quality and productivity performance of strategies.

Strategy	***E^{Eff} [parts/t.u]***	***E^{Tot} [parts/t.u]***	***$\Delta\%$ E^{Eff} vs. curr. assembly***
Curr. assembly	0.5752	0.6729	-
Proposed assembly	0.6704	0.6704	+16.55%

In addition to the quality improvements achieved on KQC_1, significant improvements are also obtained on KQC_2. In the current strategy, there are no quantitative criteria to measure the uniformity of magnetic profile KQC_2. However, as discussed in Section 2, the variance of the magnetic flux profile is considered as a direct indicator of the magnetic flux uniformity of the rotor. For this reason, 10 replicates of experiments consisting the assembly of 200 rotors of the type $S_P = 5$, from 1000 simulated stacks are performed. The results show that the average variance of the magnetic flux across the circumference of the rotors is reduced by 66.9% for the newly proposed strategy with respect to the current strategy. A visualization of the results from these experiments is reported for a sampled case in (Fig. 11 and Fig. 12)

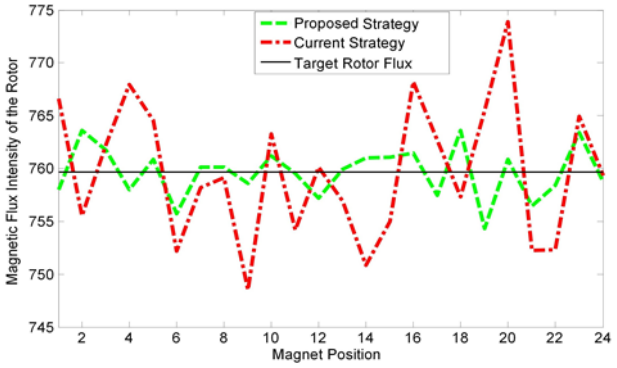

Fig. 11. Impact of the proposed strategies on uniformity of flux of one stack composed of 24 permanent magnets.

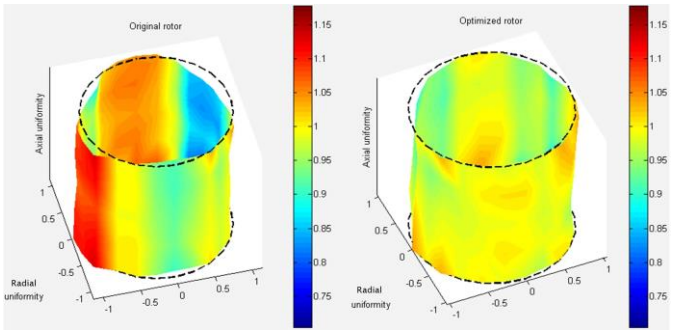

Fig. 12. 3D visualization of the field uniformity of the assembled rotor before (left) and after (right) optimization.

6. Implementation architecture and demonstration

The in-line implementation of the proposed solution requires the development and installation of hardware and software components. These installations should perform additional operations: information exchange between stations, the analysis of the input information by a computer and then the transfer of the output results to the assembly station and to the operator. Therefore, in order to validate the proposed solution, a pilot demonstration test bed is developed for verifying the method and for providing industrial implementation scheme. The final solution requires the integration of these hardware and software components into the new configuration. Thus, the hardware components that are developed for the test bed include the stack inspection test bench and an automated rotor assembly station. The software components perform the acquisition, storage and visualization of data from the inspection station. Additionally, software for the optimization and visualization of the optimal assembly solution is installed. Data communication systems integrating components into coordinated CPS systems are also implemented [41].

From a system level perspective, the new solution can be viewed as an augmentation of the assembly station through the integration with the inspection as shown in Fig. 10. However, the integration of the inspection station to the assembly station should be based on an architecture that guarantees the

requirements for information exchange, the analysis of this input information by a computer and then the transfer of the output results to the assembly station. The proposed schema is presented in Fig. 13. The inspection station acquires the space resolved magnetic profile of measured stacks and sends this data to the in-line computer. Once the in-line computer has the space resolved measurements about the stacks in the buffer, it performs the transformation and estimation of stack flux as presented in section 3. Then the optimization algorithm provides the solution for the optimal assembly by considering both KQC_1, and KQC_2. The output information includes; instructions on the choice of the stacks to be assembled from the buffer based on KQC_1, and then their rotational and vertical alignments based on KQC_2. These instructions are displayed on a screen using a simplified HMI for stack representation and a 3D visualization of the magnetic profile uniformity of the assembled rotor. This information allows sequencing and radially arranging the stacks to be assembled by a pneumatically operated mechanism at the final assembly station. The scheme demonstrating the implementation of individual developments and their integration is shown Fig. 13.

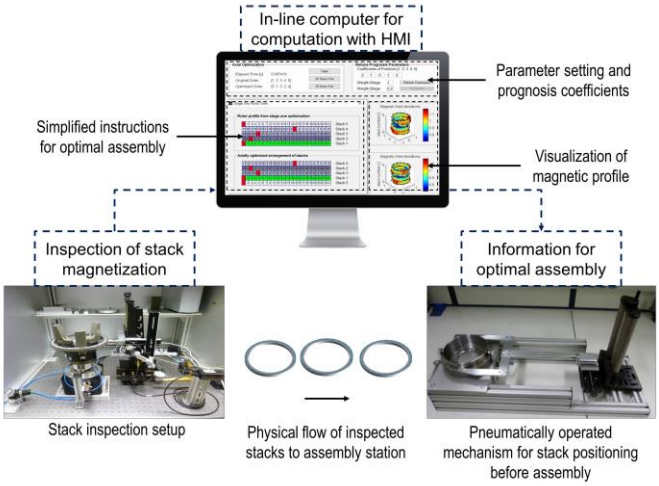

Fig. 13. Implementation schema of the new CPS based assembly station.

The actual implementation setting of the demonstrator into an integrated station including the inspection station, optimization tool and assembly mechanism is shown below.

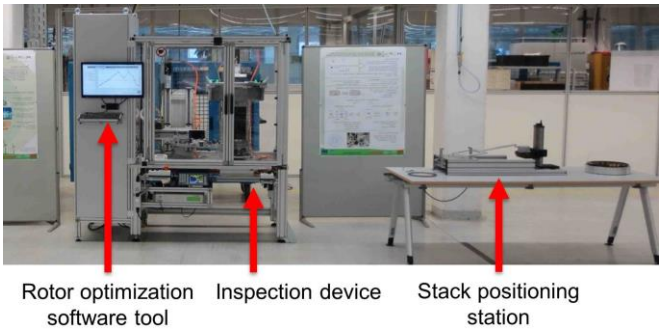

Fig. 14. Demonstration of the proposed solution implemented into stations.

7. Conclusion and prospects

This paper proposes a new quality-oriented assembly strategy for the reduction of defects in multi-stage production lines for rotor manufacturing in the automotive industry. The selection of the stacks and the assembly process are adjusted depending on the in-line measurements of the output of the magnetization process, under a cyber-physical system architecture. A methodology to support the design of the best possible strategy by estimating the impact on the overall system performance was developed. The benefits of the approach are demonstrated within a real industrial process-chain, dedicated to the production of electric motors. Simulated experiments under similar conditions indicate a system level improvement of 16.5% in the number of conforming rotors, and an average reduction of 66.9% on the variability of magnetic flux.

Generalizations and extensions of the proposed methodologies can be applied to systems in several industrial contexts where emerging technologies are adopted, such as, the production of Li-Ion batteries in the automotive industry. The proposed strategy and software solution helps facilitating the achievement of zero defect propagation solutions by correcting the defect before it reaches the end-of-line.

Acknowledgements

The research leading to these results has received funding from the European Union Seventh Framework Program (FP7/2007-2011) under grant agreement n° 285075 in the project MuProD, which is part of the 4ZDM Cluster.

References

[1] European Commission, 2011. Communication from the Commission to the European Parliament, the Council, the European Economic and Social Committee and the Committee of the Regions: A Roadmap for moving to a competitive low carbon economy in 2050.

[2] IEA, 2015. Co2 emissions from fuel combustion 2015. International Energy Agency, Paris.

[3] Greene, D.L., Park, S., Liu, C., 2014. Analyzing the transition to electric drive vehicles in the U.S. Futures 58, 34–52.

[4] Plötz, P., Schneider, U., Globisch, J., Dütschke, E., 2014. Who will buy electric vehicles?: Identifying early adopters in Germany. Transportation Research Part A: Policy and Practice 67, 96–109.

[5] European Commission (EC), 2011. Interim Assessment of the Research PPPs in the European Economic Recovery Plan, Energy Efficient Building, Factories of the Future, European Green Cars Initiative.

[6] IEA, 2016. Global EV Outlook 2016: Beyond one million electric cars. International Energy Agency (IEA), Paris, 51 pp. https://www.iea.org/publications/freepublications/publication/Global_EV_Outlook_2016.pdf. Accessed 13 April 2017.

[7] Butov, A., Verl, A., 2014. Comparison of end of line tests for serial production of electric motors in hybrid truck applications, in: Proceedings of the 4th International Electric Drives Production Conference (EDPC), Nürnberg. 30. September - 01. Oktober 2014, pp. 1–4.

[8] Meyer, A., Heyder, A., Kühl, A., Sand, C., Gehb, H., Abersfelder, S., Franke, J., Holzhey, R., Büttner, U., Wangemann, S., 2016. Concept for Magnet Intra Logistics and Assembly Supporting the Improvement of Running Characteristics of Permanent Magnet Synchronous Motors. Procedia CIRP 43, 356–361.

[9] Cassing, W., Kunzte, K., Ross, G., 2015. Dauermagnete: Mess- und Magnetisiertechnik, 2., neu bearb. Aufl. ed. Expert-Verlag, Renningen, 244 S.

[10] Dudding, J., Knell, P.A., Cornelius, R.N., Enzberg-Mahlke, B., Fernengel, W., Grössinger, R., Küpferling, M., Lethuillier, P., Reyne, G., Taraba, M., Toussaint, J.C., Wimmer, A., Edwards, D., 2002. A pulsed

field magnetometer for the qualitiy control of permanent magnets. Journal of Magnetism and Magnetic Materials 242-245, 1402–1404.
[11] Grössinger, R., 2008. Characterisation of hard magnetic materials. J. Electrical Engineering 59, 15–20.
[12] Rothwarf, F., Simizu, S., Huang, M.Q., Schaefer, R.J., 1993. Pulsed field magnetometer for nondestructive monitoring of encapsulated magnetic materials. Journal of Applied Physics 73 (10), 5614–5616.
[13] Song, M.-S., Kim, Y.-B., Kim, C.-S., Kim, T.-K., 2000. Measurement accuracy of a pulsed field magnetometer designed for rare earth based permanent magnets. IEEE Trans. Magn. 36 (5), 3637–3639.
[14] Schlechtendahl, J., Kretschmer, F., Sang, Z., Lechler, A., Xu, X., 2015. Extended study of network capability for cloud based control systems. Robotics and Computer-Integrated Manufacturing.
[15] Monostori, L., Kádár, B., Bauernhansl, T., Kondoh, S., Kumara, S., Reinhart, G., Sauer, O., Schuh, G., Sihn, W., Ueda, K., 2016. Cyber-physical systems in manufacturing. CIRP Annals - Manufacturing Technology 65 (2), 621–641.
[16] Lee, J., Bagheri, B., Kao, H.-A., 2015. A Cyber-Physical Systems architecture for Industry 4.0-based manufacturing systems. Manufacturing Letters 3, 18–23.
[17] Harrison, R., Vera, D., Ahmad, B., 2016. Engineering Methods and Tools for Cyber–Physical Automation Systems. Proc. IEEE 104 (5), 973–985.
[18] Brettel, M., Friederichsen, N., Keller, M., Rosenberg, M., 2014. How virtualization, decentralization and network building change the manufacturing landscape: An Industry 4.0 Perspective. International Journal of Mechanical, Industrial Science and Engineering 8 (1), 37–44.
[19] Verl, A., Lechler, A., Wesner, S., Kirstädter, A., Schlechtendahl, J., Schubert, L., Meier, S., 2013. An Approach for a Cloud-based Machine Tool Control. Procedia CIRP 7, 682–687.
[20] Coupek, D., Friedrich, J., Verl, A., Lechler, A., 2014. Modular Information Sharing Platform for Real-Time Data Processing and Knowledge Extraction in Modern Production Systems, in: Proceedings of the International Conference Management of Technology – Step to Sustainable Production (MOTSP), Bol, Croatia. 11. - 13. Juni 2014, pp. 1–8.
[21] Coupek, D., Verl, A., Aichele, J., Colledani, M., 2013. Proactive quality control system for defect reduction in the production of electric drives, in: Proceedings of the 3rd International Electric Drives Production Conference (EDPC), Nürnberg. 29. - 30. Oktober 2013, pp. 1–6.
[22] Coupek, D., Verl, A., 2014. Ausschussreduzierung und Defektkompensation in mehrstufigen Produktionssystemen, in: Brecher, C. (Ed.), Effiziente Produktion, Als Ms. gedr ed. VDI-Verl., Düsseldorf, pp. 82–91.
[23] Butov, A., Herrmann, F., Merkert, M., Nägele, F., 2014. Modulares Fertigungskonzept für E-Motoren. Automobiltechnische Zeitschrift ATZ 116 (9), 84–88.
[24] Dorrell, D.G., Knight, A.M., Popescu, M., Evans, L., Staton, D.A., 2010. Comparison of different motor design drives for hybrid electric vehicles, in: 2010 IEEE Energy Conversion Congress and Exposition (ECCE), Atlanta, GA, USA, pp. 3352–3359.
[25] Klippel, W., 2011. End-Of-Line Testing, in: Grzechca, W. (Ed.), Assembly Line - Theory and Practice. InTech, pp. 181–206.
[26] Colledani, M., Copani, G., Tolio, T., 2014. De-manufacturing Systems. Procedia CIRP 17, 14–19.
[27] Vervaeke, K., 2011. Inline magnet inspection using fast high resolution MagCam magnetic field mapping and analysis, in: Proceedings of the 1st International Electric Drives Production Conference (EDPC), Nürnberg. 28. - 29. September 2011, pp. 172–180.
[28] König, W., 2014. Verfahren und Vorrichtung zur Überwachung eines Magnetisierungsprozesses von Magnetpolen. http://www.freepatentsonline.com/DE102014005806A1.html.
[29] Naumoski, H., Lampmann, F., 2014. Verfahren zum Überprüfen eines Rotors auf vollständige Magnetisierung. http://www.freepatentsonline.com/DE102014010644.html.
[30] Jewon Lee, Yong-Ju Jeon, Doo-chul Choi, SeungHun Kim, Kim, S.W., 2013. Demagnetization fault diagnosis method for PMSM of electric vehicle, in: IECON 2013 - 39th Annual Conference of the IEEE Industrial Electronics Society, Vienna, Austria. 10. - 13. November 2013, pp. 2709–2713.
[31] Moosavi, S.S., Djerdir, A., Amirat, Y.A., Khaburi, D.A., 2014. Demagnetization fault investigation in permanent magnet synchronous motor, in: 2014 5th Power Electronics, Drive Systems & Technologies Conference (PEDSTC), Tehran, Iran. 05. - 06. Februar 2014, pp. 617–623.
[32] Koschny, M., Lindner, M., 2016. Magische Momente beim Visualisieren von Magnetfeldern. Werkstoffzeitschrift. http://werkstoffzeitschrift.de/magische-momente-beim-visualisieren-von-magnetfeldern/. Accessed 13 April 2017.
[33] Michalowsky, L. (Ed.), 2006. Magnettechnik: Grundlagen, Werkstoffe, Anwendungen, 3. aktualisierte Aufl. ed. Vulkan-Verl., Essen, XIV, 366.
[34] Popović, R.S., 2004. Hall effect devices, 2nd ed. ed. Institute of Physics Pub, Bristol, Philadelphia, xvi, 419.
[35] Ramsden, E., 2006. Hall-effect sensors: Theory and applications, 2nd ed. ed. Elsevier/Newnes, Amsterdam, Boston.
[36] Tremel, J., Franke, J., 2012. Hall sensor line array for magnetic field inline measurements of PM-exited rotors, in: Proceedings of the 2nd International Electric Drives Production Conference (EDPC), Nürnberg. 15. -18. Oktober 2012, pp. 1–4.
[37] Coupek, D., Verl, A., Lechler, A., Aichele, J., Junker, S., 2014. Defect reduction in the production of electric drives by downstream compensation and space-resolved inspection, in: Proceedings of the 4th International Electric Drives Production Conference (EDPC), Nürnberg. 30. September - 01. Oktober 2014, pp. 1–8.
[38] Colledani, M., Tolio, T., 2011. Integrated analysis of quality and production logistics performance in manufacturing lines. International Journal of Production Research 49 (2), 485–518.
[39] Tan, B., Gershwin, S.B., 2009. Analysis of a general Markovian two-stage continuous-flow production system with a finite buffer. International Journal of Production Economics 120 (2), 327–339.
[40] Colledani, M., Tolio, T., 2006. Impact of Quality Control on Production System Performance. CIRP Annals - Manufacturing Technology 55 (1), 453–456.
[41] Coupek, D., Lechler, A., Verl, A., 2016. Cloud-based control for downstream defect reduction in the production of electric motors, in: Proceedings of the International Conference on Electrical Systems for Aircraft, Railway, Ship Propulsion and Road Vehicles & International Transportation Electrification Conference (ESARS-ITEC), Toulouse, France. 02. - 04. November 2016, pp. 1–6.